A MULTIGRID SOLVER FOR THE STEADY STATE NAVIER-STOKES EQUATIONS USING THE PRESSURE-POISSON FORMULATION

DAVID SIDILKOVER* AND URI M. ASCHER†

Abstract. This paper presents an efficient multigrid solver for steady-state Navier-Stokes equations in 2D on non-staggered grids. The pressure Poisson equation formulation is used, together with a finite volume discretization. A discretization of the boundary conditions for pressure and velocities is presented. An efficient multigrid algorithm for solving the resulting discrete equations is then developed. The issue of the numerical treatment of advection is also addressed: a family of stable and accurate difference schemes for the advection-dominated flow are presented. This family includes also second order accurate schemes.

1. Introduction. The steady-state incompressible Navier-Stokes equations in two dimensions can be written in the following *primitive* form

$$-\nu\Delta\mathbf{u} + (\mathbf{u}\cdot\nabla)\mathbf{u} + \nabla p = \mathbf{s} \tag{1.1}$$

$$\nabla\cdot\mathbf{u} = \mathbf{0} \tag{1.2}$$

where $\mathbf{u}(\mathbf{x})$ is the velocity field at $\mathbf{x}$; $p(\mathbf{x})$ is the kinematic pressure; $\nu \geq 0$ is the kinematic viscosity; and $\mathbf{s}(\mathbf{x})$ is an external force. Here we consider a boundary-value problem for (1.1)-(1.2) in a domain $\bar{\Omega} \equiv \Omega \cup \Gamma$ with the boundary conditions considered in [4]

$$\mathbf{u}(\mathbf{x}) = \mathbf{w} \qquad \text{on} \quad \Gamma_D \tag{1.3}$$

$$-p + \nu\partial u_n/\partial n = F_n \quad \text{and} \quad \nu\partial u_\tau/\partial n = F_\tau \qquad \text{on} \quad \Gamma_N, \tag{1.4}$$

where $\Gamma = \Gamma_D \cup \Gamma_N$, n stands for normal component and outward normal direction, and τ stands for tangential component and tangential direction. If (and only if) $\Gamma = \Gamma_D$ ($\Gamma_N = \emptyset$), then $\mathbf{w}$ must satisfy the following solvability condition

$$\int_\Gamma \mathbf{n}\cdot\mathbf{w} = 0. \tag{1.5}$$

There exist several approaches towards discretizing the incompressible Navier-Stokes equations. Efficient multigrid solvers based on the staggered grid discretization of the system (1.1),(1.2) were developed, e.g., in [2],[1],[14].

However, there are reasons why a discretization on a non-staggered grid is desirable. These include simpler procedures, at least conceptually, for local grid refinement, treatment of complex geometries and design of good smoothers. Especially in 3-D, this may prove useful in reducing programmer's headaches considerably. It is well known that an attempt to discretize the system (1.1),(1.2) on a non-staggered grid using central differences to approximate the pressure derivatives and the continuity equation leads to a discrete system suffering from spurious modes in the pressure solution. A possible remedy can be to approximate pressure derivatives and the continuity equation by one-sided differences oriented in a certain way (see [3]). However, the accuracy in this case will degrade to first order.

* Courant Institute of Mathematical Sciences, New York University, New York, NY 10012, USA

† Department of Computer Science, University of British Columbia, Vancouver, BC, V6T 1Z2, Canada.
The work of this author was partially supported under NSERC Canada Grant OGP0004306.

We adopt here a Pressure Poisson Equation formulation (PPE) of the Navier-Stokes equations. The equation for pressure can be obtained by taking a divergence of (1.1) and applying (1.2) (see, for instance, [5]), yielding

$$\Delta p = -\nabla \cdot (\mathbf{u} \cdot \nabla)\mathbf{u} + \nabla \cdot \mathbf{s} \qquad \text{in} \quad \Omega \tag{1.6}$$

The obtained system (1.1),(1.6) can be sensibly discretized on a nonstaggered grid. However, the differential order of the system (1.1),(1.6) is higher than that of the primitive system (1.1),(1.2). Additional boundary conditions should therefore be specified in order to make the problem well-posed, and it is well-known that a careful specification and discretization of these additional conditions can be crucial for the performance of the resulting algorithm, especially in the viscous case.

The boundary conditions for pressure considered in [4] are the following

$$\frac{\partial p}{\partial n} = \mathbf{n} \cdot (\nu \Delta \mathbf{u} + \mathbf{s} - \mathbf{u} \cdot \nabla \mathbf{u}) \qquad \text{on} \quad \Gamma_D \tag{1.7}$$

$$p = \nu \frac{\partial u_n}{\partial n} - F_n \qquad \text{on} \quad \Gamma_N. \tag{1.8}$$

It is shown in [5] that for the case $\Gamma_N = \emptyset$ and $\Gamma_D = \Gamma$ the corresponding Neumann problem for p is well-posed (with a unique solution up to an arbitrary additive constant) if $\mathbf{w}$ satisfies the solvability constraint (1.5).

Here we consider directly two cases:

- The viscous case ($\nu > 0$), with $\Gamma = \Gamma_D$ ($\Gamma_N = \emptyset$). The well-posed problem under consideration is then (1.1),(1.6),(1.3),(1.7).
- The inviscid case ($\nu = 0$), with Γ_D representing the inflow boundary and Γ_N – the outflow boundary.
  The high (though finite) Reynolds number case can be considered under this category as well, using the *parabolized* Navier-Stokes equations (see [11]).

We show how to treat such a coupled system efficiently, using a multigrid method applied to a careful discretization scheme.

The paper is organized as follows: In §2 we describe an efficient multigrid solver for the PPE with Neumann boundary conditions. We present a scheme to discretize the pressure boundary conditions for both inviscid and viscous cases. This is followed in §3 by a description of accurate and stable discretization schemes for the momentum equations for the entire range of Reynolds number. In §4 we describe the overall multigrid algorithm for solving the obtained discrete system of equations and in §5 we present numerical experiments. All this is followed by a discussion of the current state of the algorithms and possible future developments.

For the rest of this paper, we restrict the discussion to two space dimensions.

2. Discretization of the PPE and the pressure boundary conditions. At first, consider a Poisson equation

$$\Delta p = f(x) \qquad \text{in} \quad \Omega \tag{2.1}$$

subject to Neumann boundary conditions

$$\frac{\partial p}{\partial n} = g(x) \qquad \text{on} \quad \Gamma \tag{2.2}$$

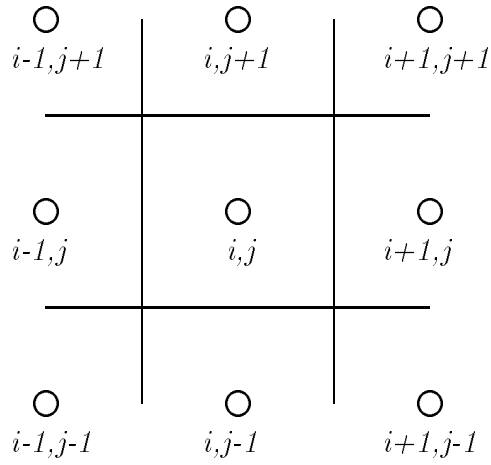

FIG. 2.1. *Interior control volume.*

The following relation between f and g should hold

$$\oint_\Gamma \frac{\partial p}{\partial n} ds \equiv \oint_\Gamma g \, ds = \int\int_\Omega f(x,y) dx dy \tag{2.3}$$

in order to allow for solution existence. We shall refer to (2.3) as the *compatibility condition.*

Assume Ω to be a rectangular domain so that $\frac{\partial p}{\partial n}$ is either p_x or p_y on the boundary.

Recall the discretization of the Poisson equation using a finite volume approach (see, e.g. [8]):

At an *interior* grid point (i,j) consider a volume as shown in Fig.2.1. Integrating $\Delta p = \nabla(\nabla p)$ and using the divergence theorem gives

$$h[(p_x)_{i+\frac{1}{2},j} - (p_x)_{i-\frac{1}{2},j}] + h[(p_y)_{i,j+\frac{1}{2}} - (p_y)_{i,j-\frac{1}{2}}] = h^2 f_{i,j}$$

and further using centered differences gives the usual formula

$$-4p_{i,j} + p_{i+1,j} + p_{i-1,j} + p_{i,j+1} + p_{i,j-1} = h^2 f_{i,j}$$

At a *boundary* point, say $(i,0)$, consider a volume as shown in Fig.2.2. (Thus, for i not a boundary the volume is half the one for the interior.) Integration of Δp now gives using (2.1)

$$h[(p_x)_{i+\frac{1}{2},0} - (p_x)_{i-\frac{1}{2},0}] + 2h[(p_y)_{i,\frac{1}{2}} - (p_y)_{i,0}] = h^2 f_{i,0}$$

or, using (2.2) for $(p_y)_{i,0}$,

$$-4p_{i,0} + p_{i+1,0} + p_{i-1,0} + 2p_{i,1} = h^2 f_{i,0} - 2hg_{i,0}.$$

Considering a *corner* point we obtain

$$2h[(p_x)_{\frac{1}{2},0} - (p_x)_{0,0}] + 2h[(p_y)_{0,\frac{1}{2}} - (p_y)_{0,0}] = h^2 f_{0,0}$$

or

$$-4p_{0,0} + 2p_{1,0} + 2p_{0,1} = h^2 f_{0,0} + 2h(p_x)_{0,0} + 2h(p_y)_{0,0},$$

where $(p_x)_{0,0}$ and $(p_y)_{0,0}$ are again given by (2.2).

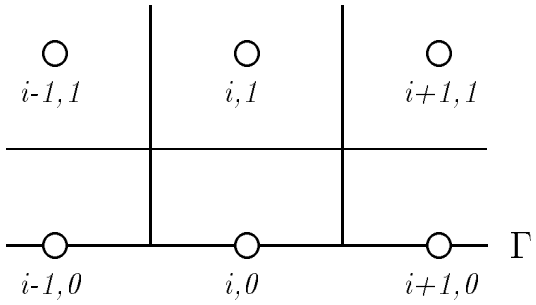

FIG. 2.2. *Boundary control volume.*

Remark 1 Note that even though the compatibility condition (2.3) holds on the continuous level, a small-magnitude incompatibility may arise on the discrete level. Therefore, when solving the discrete equations by an iterative method like Gauss-Seidel one may observe in general that the residuals do not decrease below a certain level. However, since the discrete incompatibility is due to the discretization error, the level at which the residuals stop decreasing is at that of the desired accuracy. Alternatively, an adjustment to the inhomogeneities can be made to ensure discrete compatibility, which allows convergence of Gauss-Seidel to vanishing residuals, but which does not increase the accuracy of the obtained solution. □

A standard multigrid algorithm using, say, red-black Gauss-Seidel relaxation and the usual bilinear interpolation and its adjoint for prolongation and restriction, respectively, can now be applied. The obtained efficiency is comparable to the excellent efficiency of the same method for Poisson's equation with Dirichlet boundary conditions.

Turning to the equation for pressure (1.6), we write it in the following form

$$\Delta p + 2(v_x u_y - u_x v_y) = s^u_x + s^v_y \tag{2.4}$$

where $(s^u, s^v) = \mathbf{s}$. This can be discretized using the finite volume approach as follows

$$\begin{aligned} &-4p_{i,j} + p_{i+1,j} + p_{i-1,j} + p_{i,j+1} + p_{i,j-1} \\ &+\frac{1}{2}((v_{i+1,j} - v_{i-1,j})(u_{i,j+1} - u_{i,j-1}) - (u_{i+1,j} - u_{i-1,j})(v_{i,j+1} - v_{i,j-1})) \\ &= h^2((s^u_x)_{i,j} + (s^v_y)_{i,j}) \end{aligned} \tag{2.5}$$

where the derivatives s^u_x and s^v_y can be either computed analytically or approximated by finite differences.

At a *boundary* point which is not a corner point, say $(i, 0)$, integration of Δp now gives

$$h[(p_x)_{i+\frac{1}{2},0} - (p_x)_{i-\frac{1}{2},0}] + 2h[(p_y)_{i,\frac{1}{2}} - (p_y)_{i,0}] = 2h^2(u_x v_y - v_x u_y)_{i,0} + h^2((s^u_x)_{i,0} + (s^v_y)_{i,0})$$

or

$$\begin{aligned} &-4p_{i,0} + p_{i+1,0} + p_{i-1,0} + 2p_{i,1} = \\ &[(u_{i,1} - u_{i,0})(v_{i+1,0} - v_{i-1,0}) - (u_{i+1,0} - u_{i-1,0})(v_{i,1} - v_{i,0})] \\ &+2 \cdot h(p_y)_{i,0} + h^2((s^u_x)_{i,0} + (s^v_y)_{i,0}) \end{aligned} \tag{2.6}$$

and a similar derivation is carried out for a corner point. The complication, compared to the simple problem with (2.2), is in deriving appropriate expressions for $(p_y)_{i,0}$. To simplify notation, we assume from now on that $\mathbf{s} \equiv \mathbf{0}$.

2.1. Pressure boundary conditions: inviscid case. For p_y we use the momentum and the continuity equations as in (1.7),

$$p_y = -uv_x - vv_y = -uv_x + vu_x \tag{2.7}$$

Discretizing this at the point $(i, 0)$ gives

$$(p_y)_{i,0} = -u_{i,0}\frac{v_{i+1,0} - v_{i-1,0}}{2h} + v_{i,0}\frac{u_{i+1,0} - u_{i-1,0}}{2h} \tag{2.8}$$

We see that the pressure boundary condition does not depend on the internal velocity values. Therefore, this case can be reduced to the previously described case of Poisson equation with Neumann boundary conditions without difficulty.

2.2. Pressure boundary conditions: viscous case. Assume $\Gamma_D = \Gamma$ and consider the Neumann problem for the PPE (1.6),(1.7). It is easy to see that the compatibility condition (2.3) is satisfied in this case provided the continuity equation (1.2) holds.

At the bottom boundary of our rectangular domain, (1.7) reads

$$p_y = \nu\Delta v - uv_x - vv_y = \nu\Delta v - uv_x + vu_x \tag{2.9}$$

Denoting the quantity on the right hand side of (2.8) by $(\bar{p}_y)_{i,0}$, we now have

$$(p_y)_{i,0} = \nu\frac{((v_x)_{i+\frac{1}{2},0} - (v_x)_{i-\frac{1}{2},0}) + 2((v_y)_{i,\frac{1}{2}} - (v_y)_{i,0})}{h} + (\bar{p}_y)_{i,0}$$

Using the continuity equation we get

$$(p_y)_{i,0} = \nu\frac{((v_x)_{i+\frac{1}{2},0} - (v_x)_{i-\frac{1}{2},0}) + 2((v_y)_{i,\frac{1}{2}} + (u_x)_{i,0})}{h} + (\bar{p}_y)_{i,0}$$

Discretizing this and substituting into (2.6) gives

$$\begin{aligned}
&-4p_{i,0} + p_{i+1,0} + p_{i-1,0} + 2p_{i,1} = \\
&[(u_{i,1} - u_{i,0})(v_{i+1,0} - v_{i-1,0}) - (u_{i+1,0} - u_{i-1,0})(v_{i,1} - v_{i,0})] \\
&+\frac{2\nu}{h}[(v_{i+1,0} - 2v_{i,0} + v_{i-1,0}) + 2(v_{i,1} - v_{i,0}) + (u_{i+1,0} - u_{i-1,0})] \\
&+v_{i,0}(u_{i+1,0} - u_{i-1,0}) - u_{i,0}(v_{i+1,0} - v_{i-1,0})
\end{aligned} \tag{2.10}$$

Remark 2 Note that while (2.3) holds, discrete compatibility in general holds only up to discretization error level, and Remark 1 applies. □

3. Discretization of the momentum equations. We present in this section a discretization scheme for the homogeneous u-momentum equation only, namely,

$$-\nu\nabla^2 u + uu_x + vu_y + p_x = 0. \tag{3.1}$$

The v-momentum equation can be treated in a similar way, and the treatment of force terms is obvious.

3.1. A hybrid scheme for the general case. Denote the discrete operator representing the u-momentum equation by

$$
\begin{aligned}
L_h^u &= \frac{u_{i,j}(u_{i+1,j}-u_{i-1,j})+v_{i,j}(u_{i,j+1}-u_{i,j-1})}{2h} \\
&+ \frac{p_{i+1,j}-p_{i-1,j}}{2h} \\
&- \frac{(F_{i+\frac{1}{2},j}-F_{i-\frac{1}{2},j})+(G_{i,j+\frac{1}{2}}-G_{i,j-\frac{1}{2}})}{h}.
\end{aligned} \tag{3.2}
$$

Here F and G are the viscous fluxes

$$
\begin{aligned}
F_{i-\frac{1}{2},j} &= F^p_{i-\frac{1}{2},j} + \xi_{i-\frac{1}{2},j} \cdot F^a_{i-\frac{1}{2},j} \\
G_{i,j-\frac{1}{2}} &= G^p_{i,j-\frac{1}{2}} + \eta_{i,j-\frac{1}{2}} \cdot G^a_{i,j-\frac{1}{2}}
\end{aligned} \tag{3.3}
$$

where F^p, G^p denote the fluxes due to the physical viscosity

$$
\begin{aligned}
F^p_{i-\frac{1}{2},j} &= \nu \frac{u_{i,j}-u_{i-1,j}}{h} \\
G^p_{i,j-\frac{1}{2}} &= \nu \frac{u_{i,j}-u_{i,j-1}}{h},
\end{aligned} \tag{3.4}
$$

$$
\xi_{i-\frac{1}{2},j} = \max\{0, \frac{|u_{i-\frac{1}{2},j}| - 2\nu/h}{|u_{i-\frac{1}{2},j}|}\}; \quad \eta_{i,j-\frac{1}{2}} = \max\{0, \frac{|v_{i,j-\frac{1}{2}}| - 2\nu/h}{|v_{i,j-\frac{1}{2}}|}\} \tag{3.5}
$$

$$
u_{i-\frac{1}{2},j} = \frac{u_{i,j}+u_{i-1,j}}{2}; \quad v_{i-\frac{1}{2},j} = \frac{v_{i,j}+v_{i-1,j}}{2}; \tag{3.6}
$$

$$
u_{i,j-\frac{1}{2}} = \frac{u_{i,j}+u_{i,j-1}}{2}; \quad v_{i,j-\frac{1}{2}} = \frac{v_{i,j}+v_{i,j-1}}{2}; \tag{3.7}
$$

and F^a, G^a denote the artificial viscosity fluxes. It can be easily shown that (3.2) approximates (3.1) with second order accuracy in the centered case when $\xi_{i-\frac{1}{2},j}, \eta_{i,j-\frac{1}{2}} = 0$. The case of advection-dominated flow (when $\xi_{i-\frac{1}{2},j} > 0$ or $\eta_{i,j-\frac{1}{2}} > 0$) is more difficult. The artificial viscosity fluxes should be constructed in such a way that the resulting dicretization will be stable and accurate. The rest of this section is devoted to this objective.

3.2. Advection dominated flow. We now develop several possible ways to discretize the advection part of the u-momentum equation, considering the pressure derivative as an inhomogeneity.

3.2.1. Upwind scheme. The simplest way to obtain a stable scheme is to define the artificial viscosity fluxes $F^a_{i-\frac{1}{2},j}$ and $G^a_{i,j-\frac{1}{2}}$ in the following way

$$
\begin{aligned}
F^u_{i-\frac{1}{2},j} &= \tfrac{1}{2}|u_{i-\frac{1}{2},j}|(u_{i,j}-u_{i-1,j}) \\
G^u_{i,j-\frac{1}{2}} &= \tfrac{1}{2}|v_{i,j-\frac{1}{2}}|(u_{i,j}-u_{i,j-1}).
\end{aligned} \tag{3.8}
$$

This choice obviously leads to a first order upwind scheme. The advantage of this well-known scheme is its stability, due to the artificial diffusion it introduces, but its accuracy is low. In addition to its general low order it may have significant cross-stream error. Below we therefore proceed to update this scheme further by adding terms to it in order to improve the accuracy without losing the stability.

3.2.2. Upwind narrow schemes I. A scheme with smaller cross-stream diffusion (though still first order accurate) is given by the following choice of the artificial viscosity fluxes

$$
\begin{aligned}
F^N_{i-\frac{1}{2},j} &= F^u_{i-\frac{1}{2},j} + \tfrac{1}{2} s^u_{i-\frac{1}{2},j} \beta_{i-\frac{1}{2},j} |v_{i-\frac{1}{2},j}| (\delta_y u)_{i-\frac{1}{2},j} \\
G^N_{i,j-\frac{1}{2}} &= G^u_{i,j-\frac{1}{2}} + \tfrac{1}{2} s^v_{i,j-\frac{1}{2}} \alpha_{i,j-\frac{1}{2}} |u_{i-\frac{1}{2},j}| (\delta_x v)_{i,j-\frac{1}{2}},
\end{aligned} \tag{3.9}
$$

where

$$
\beta_{i-\frac{1}{2},j} = \min(1, \frac{|u_{i-\frac{1}{2},j}|}{|v_{i-\frac{1}{2},j}|}) \qquad \alpha_{i,j-\frac{1}{2}} = \min(1, \frac{|v_{i,j-\frac{1}{2}}|}{|u_{i,j-\frac{1}{2}}|}), \tag{3.10}
$$

$$
s^u_{i-\frac{1}{2},j} = \mathrm{sign}(u_{i-\frac{1}{2},j}) \qquad s^v_{i-\frac{1}{2},j} = \mathrm{sign}(v_{i-\frac{1}{2},j}) \tag{3.11}
$$

$$
s^u_{i,j-\frac{1}{2}} = \mathrm{sign}(u_{i,j-\frac{1}{2}}) \qquad s^v_{i,j-\frac{1}{2}} = \mathrm{sign}(v_{i,j-\frac{1}{2}}) \tag{3.12}
$$

$$
(\delta_y u)_{i-\frac{1}{2},j} = \begin{cases} u_{i-1,j} - u_{i-1,j-(s^v_{i-\frac{1}{2},j})}, & \text{if } u_{i-\frac{1}{2},j} \geq 0 \\ u_{i,j} - u_{i,j-(s^v_{i-\frac{1}{2},j})}, & \text{if } u_{i-\frac{1}{2},j} < 0 \end{cases} \tag{3.13}
$$

and

$$
(\delta_x v)_{i,j-\frac{1}{2}} = \begin{cases} v_{i,j-1} - v_{i-(s^u_{i,j-\frac{1}{2}}),j-1}, & \text{if } v_{i,j-\frac{1}{2}} \geq 0 \\ v_{i,j} - v_{i-(s^u_{i,j-\frac{1}{2}}),j}, & \text{if } v_{i,j-\frac{1}{2}} < 0 \end{cases} \tag{3.14}
$$

This scheme is very similar to one presented in [9]. It was also presented in [13], where it was named the N scheme (because of the narrow stencil). A detailed analysis of its properties is given in [10].

3.2.3. Upwind narrow schemes II. The compact schemes developed for a scalar advection equation can be viewed as the regular upwind scheme with some additional first order small terms added in such a way that when grouped together with the first order error terms of the upwind scheme they will cancel each other (at least in part) due to the original advection equation itself. However, here we deal with the Navier-Stokes system of differential equations. We can use any of these equations to achieve the desired error cancellation when approximating, say, the first momentum equation.

This observation leads to another upwind narrow scheme

$$
\begin{aligned}
F^{NC}_{i-\frac{1}{2},j} &= F^u_{i-\frac{1}{2},j} + \tfrac{1}{2} |u_{i-\frac{1}{2},j}| (\delta_y v)_{i-\frac{1}{2},j} \\
G^{NC}_{i,j-\frac{1}{2}} &= G^N_{i,j-\frac{1}{2}}
\end{aligned} \tag{3.15}
$$

Here the continuity equation (1.2) is used to achieve error cancellation for F-fluxes. This NC-scheme is simpler than the N-scheme above.

3.2.4. Zero cross-diffusion schemes. An even better scheme is given by the following choice of the artificial viscosity fluxes

$$
\begin{aligned}
F^Z_{i-\frac{1}{2},j} &= F^N_{i-\frac{1}{2},j} - \tfrac{1}{2}(1-\beta_{i-\frac{1}{2},j})|v_{i-\frac{1}{2},j}|(u_{i-1,j-s^v_{i-\frac{1}{2},j}} - u_{i,j-s^v_{i-\frac{1}{2},j}}) \\
G^Z_{i,j-\frac{1}{2}} &= G^N_{i,j-\frac{1}{2}} - \tfrac{1}{2}(1-\alpha_{i,j-\frac{1}{2}})|u_{i,j-\frac{1}{2}}|(u_{i-s^u_{i,j-\frac{1}{2},j}} - u_{i-s^u_{i,j-\frac{1}{2},j-1}}).
\end{aligned} \tag{3.16}
$$

This scheme, which was first proposed in [7], is called a zero cross-diffusion scheme because its cross-stream truncation error component is second order small. It can also be obtained as a particular case of the scheme presented in [12],[13]. A detailed analysis of the family of zero cross-diffusion schemes is given in [6]. These schemes give a second order accurate solution for a homogeneous steady-state advection equation.

Again we now recall that the solution sought satisfies not just an advection equation but the entire Navier-Stokes system. An alternative zero cross-diffusion scheme (using the correction term based on the continuity equation for F fluxes) can be given by the following artificial viscosity fluxes

$$
\begin{aligned}
F^{ZC}_{i-\frac{1}{2},j} &= F^{NC}_{i-\frac{1}{2},j} \\
G^{ZC}_{i,j-\frac{1}{2}} &= G^Z_{i,j-\frac{1}{2}}
\end{aligned} \tag{3.17}
$$

3.2.5. Second order scheme. Each momentum equation can be viewed as a steady advection equation with inhomogeneity (pressure derivative). Therefore, in order to achieve a second order accuracy in this case, the scheme (3.16) has to be modified. This can be done by the following choice of the artificial viscosity fluxes

$$
\begin{aligned}
F^T_{i-\frac{1}{2},j} &= F^Z_{i-\frac{1}{2},j} - \tfrac{1}{2}s^u_{i-\frac{1}{2},j}\beta_{i-\frac{1}{2},j}(p_{i,j} - p_{i-1,j}) \\
G^T_{i,j-\frac{1}{2}} &= G^Z_{i,j-\frac{1}{2}} - \tfrac{1}{2}s^v_{i,j-\frac{1}{2}}\alpha_{i,j-\frac{1}{2}}(\delta_x p)_{i,j-\frac{1}{2}},
\end{aligned} \tag{3.18}
$$

where

$$
(\delta_x p)_{i,j-\frac{1}{2}} = \begin{cases} p_{i,j} - p_{i-(s^u_{i,j-\frac{1}{2}}),j}, & \text{if } v_{i,j-\frac{1}{2}} < 0 \\ p_{i,j-1} - p_{i-(s^u_{i,j-\frac{1}{2}}),j-1}, & \text{if } v_{i,j-\frac{1}{2}} \geq 0 \end{cases} \tag{3.19}
$$

The second order accuracy of this scheme follows from the fact that the first order truncation error terms vanish when substituting (3.1).

A simpler second order accurate scheme is given by the following arificial viscosity fluxes

$$
\begin{aligned}
F^{TC}_{i-\frac{1}{2},j} &= F^{NC}_{i-\frac{1}{2},j} \\
G^{TC}_{i,j-\frac{1}{2}} &= G^T_{i,j-\frac{1}{2}}
\end{aligned} \tag{3.20}
$$

The second order accuracy of this scheme follows from the fact that the first order truncation error terms vanish when substituting (3.1) and (1.2).

Among the second order schemes the TC-scheme is preferable over the T-scheme because it is significantly simpler.

Note that all of the schemes presented in this section are nonconservative. This is because the scheme (3.2) is nonconservative, approximating the differential equation (3.1), which is written in nonconservative (quasilinear) form (as is (1.1)). It is possible to generalize the construction presented here so that the resulting scheme will be conservative. However, this is not our concern here (see §6).

4. Multigrid algorithm for the steady state, incompressible Navier-Stokes equations. The multigrid algorithm implemented in order to efficiently solve the discrete system of equations developed in the previous two sections is a relatively standard one (see, e.g., [1]). It employs a Gauss-Seidel relaxation for a smoother, with red-black ordering. (An exception is for high Reynolds number in case that the flow direction is known. In such a case an ordering that goes with the flow is preferable.) A bilinear prolongation and its adjoint full-weight restriction are used for grid transfers. This is embedded in a FAS-FMG setting.

At interior grid points the three unknowns corresponding to each grid point are relaxed simultaneously. At a point next to Γ_D the three unknowns together with the pressure unknown at the closest boundary point are relaxed simultaneously (i.e. a 4×4 system is inverted). At a point next to a corner of Γ_D a 6×6 system of equations is solved for the three unknowns at the interior grid point plus three pressure values at the corner and its neighboring corner grid points.

5. Numerical experiments. All the numerical experiments presented here were performed on the square domain $\Omega = \{(x, y) : 0 \leq x \leq 2, 0 \leq y \leq 2\}$. We use 5 levels (grids), where the meshspacing of grid k is $h_k = 2^{1-k}$, $k = 1, \ldots, 5$.

5.1. Viscous case. Here we consider the case where the Dirichlet boundary conditions for velocities are given on the entire boundary Γ (i.e. $\Gamma_D = \Gamma$).

Example 1 First we consider the following problem

$$\mathbf{s} = \mathbf{0} \quad \text{and} \quad \nu = 1, \tag{5.1}$$

with the velocity boundary conditions

$$\begin{aligned} u &= x + 2 \\ v &= 2 - y \end{aligned} \tag{5.2}$$

The solution of this problem is given by (5.2) together with

$$p = -x(\frac{x}{2} + 2) - y(\frac{y}{2} - 2). \tag{5.3}$$

It is easy to see that this solution satisfies the discrete approximation of the momentum equations (see §3) and the pressure Poisson equation with Neumann-type boundary conditions (see §2) exactly. Therefore the discrete compatibility condition is also satisfied.

The purpose of this example was to test the efficiency of our multigrid algorithm for viscous problems, and indeed a reduction of residuals by a factor of $8 - 10$ per $V(2, 1)$ cycle was observed in this case. □

Example 2

Still assuming (5.1), let the velocity boundary conditions be given by

$$\begin{aligned} u &= \sin x \cdot \sin y \\ v &= \cos x \cdot \cos y \end{aligned} \tag{5.4}$$

It can be seen that (5.4) together with

$$p = -\frac{1}{2}(\cos^2 y + sin^2 x) \tag{5.5}$$

provide the solution to the problem.

The main purpose of this example is to verify the accuracy of the algorithm. Here, after an initial rapid reduction of residuals comparable to the previous example, this reduction slows down to a halt at the discretization error level (recall Remarks 1 and 2). Table 5.1 presents the solution errors on each grid obtained after the residuals no longer decrease meaningfully. We can conclude that the second order accuracy is achieved even though the

Level	L_1 error norm		
	u	v	p
2	$.291 \cdot 10^{-2}$	$.814 \cdot 10^{-3}$	$.130 \cdot 10^{1}$
3	$.211 \cdot 10^{-3}$	$.110 \cdot 10^{-3}$	.235
4	$.290 \cdot 10^{-4}$	$.281 \cdot 10^{-4}$	$.450 \cdot 10^{-1}$
5	$.650 \cdot 10^{-5}$	$.709 \cdot 10^{-5}$	$.944 \cdot 10^{-2}$

TABLE 5.1
Solution errors

residuals do not vanish. This is similar to what is observed when solving Poisson's equation with inhomogeneous Neumann boundary conditions: since the compatibility condition is obeyed on the continuous level, the only source of the discrete incompatibility is the discretization error. Note that this phenomenon of non-vanishing residuals occurs only for the Neumann problem, i.e. in our context only when $\Gamma = \Gamma_D$.

Note that in Table 5.1 not only the velocity errors but also the pressure errors appear to be second order. We have also observed second order accuracy in the discrete divergence, i.e. in the obtained approximation for (1.2). □

Our colleague Brian Wetton has performed additional calculations with our scheme for a channel flow (periodic boundary conditions in x, Dirichlet conditions in y), obtaining similar conclusions about the second order of the method in velocity, divergence and pressure.

5.2. Large Reynolds numbers . Here we consider the inviscid limit of the momentum equations (1.1) supplemented by the pressure equation (1.6).

Example 3 Consider the following problem

$$\mathbf{s} = \mathbf{0} \quad \text{and} \quad \nu \to 0, \tag{5.6}$$

with the velocity boundary conditions on the inflow part of the boundary

$$\Gamma_D = \{0 \le x \le 2, y = 0\} \cup \{x = 0, 0 \le y \le 2\}$$

$$u = e^y \qquad v = e^x \tag{5.7}$$

and the Dirichlet boundary conditions for pressure given on the outflow part of the domain

$$\Gamma_N = \{x = 2, 0 \le y \le 2\} \cup \{0 \le x \le 2, y = 2\}$$

$$p = -e^{x+y} \tag{5.8}$$

It is easy to see then that the solution to this problem is also given by (5.7), (5.8).

The L_1 error in the u-velocity component on different grid levels obtained using different schemes to solve this problem is presented in Table 5.2. The first column corresponds to the

regular upwind scheme. The second and third columns correspond to the narrow NC and zero cross-diffusion scheme ZC, respectively. It seems from these results that neither the NC nor the ZC schemes have any advantages over the simple upwind scheme. However, we should remember that this is an "artificial" problem. The usual feature of the realistic high Reynolds number flow is that the velocity field is smoother in the streamwize direction than in the cross-stream direction. Use of the NC and ZC schemes can be advantageous in this case. The last column corresponds to the TC scheme, which clearly demonstrates second order convergence for this problem.

The multigrid efficiency for the inviscid problem deteriorates compared to the low Reynolds number case. This is because only a fraction of the desirable correction in the characteristic components (.5 for a first order scheme and .25 for a second order scheme) can be obtained from the coarse grid in this case (see [1],[14]). We do not address this issue here.

6. Discussion and future work. An efficient and accurate multigrid solver for the steady-state incompressible Navier-Stokes equations on non-staggered grids based on the pressure Poisson equation (PPE) formulation of the Navier-Stokes system was constructed. The entire range of Reynolds numbers can be handled in this way. This is possible due to the following two developments:

1. An appropriate discretization and an efficient treatment of the pressure boundary conditions have been developed.
2. A family of discretization schemes for the advection-dominated flow has been constructed.

Preliminary numerical results reported here confirm that the resulting solver is capable of producing second order accurate solutions for the entire range of Reynolds number. The efficiency of the developed solver for the viscous case is comparable to the typical multigrid efficiency for the Poisson equation. The efficiency of the algorithm for the advection-dominated flow is worse, being the same as the multigrid efficiency for the advection equation. An improvement in this case can be achieved by incorporating in the algorithm the techniques developed in [14].

Another issue left for future implementation is that of complex geometries. The discretization procedure developed here is easy to generalize to a boundary segment which is not aligned with the grid. We use the continuity equation to replace normal first derivatives at the boundary by tangential ones, which are then approximated using the given velocity boundary values. The second derivative normal to the boundary, which appears in the viscous case, is replaced by a difference quotient of first normal derivatives near the boundary and at the boundary. Only the first derivative near the boundary is further discretized in the normal direction. Local averages are now used to express everything in terms of gridpoint values.

While the methodology presented here has been applied for the steady state case, a time-dependent Navier-Stokes solver can be developed based on it (cf. [4]). An analysis of the method and its implementation in this context are planned for the near future.

Acknowledgements We have benefitted from a number of discussions with Dr. B. Wetton.

REFERENCES

[1] A. Brandt, *Multigrid techniques: 1984 Guide with applications to fluid Dynamics*, The Weizmann Institute of Science, Rehovot, Israel, 1984.

[2] A. Brandt and N. Dinar, *Multigrid solution to elliptic flow problems*, in Numerical Methods for PDE's, Academic Press, New York, 1979, pp. 53–147.

[3] L. Fuchs and H.-S. Zhao, *Solution of three-dimensional viscous incompressible flows by a multi-grid method*, Internat. J. Numer. Methods Fluids, 4 (1984), pp. 539–555.

[4] P. M. Gresho, *Some current issues relevant to the incompressible Navier-Stokes equations*, Comput. Methods Appl. Mech. Engrg., 87 (1987), pp. 201–252.

[5] P. M. Gresho and R. L. Sani, *On pressure boundary conditions for the incompressible Navier-Stokes equations*, Internat. J. Numer. Methods Fluids, 7 (1987), pp. 1111–1145.

[6] C. Hirsch, *A general analysis of two-dimensional convection schemes*, VKI Lecture Series 1991-02 on Computational Fluid Dynamics, Von Karman Institute, Brussels, Belgium, Feb. 1991.

[7] B. Koren, *Low-diffusion rotated upwind schemes, multigrid and defect correction for steady, multi-dimensional Euler flows*, Report NM-R 9021, CWI, Amsterdam, 1990.

[8] S. F. McCormick, *Multilevel Adaptive Methods for Partial Differential Equations*, SIAM, 1989.

[9] J. Rice and R. Schnipke, *A monotone streamline upwind method for convection-dominated problems*, Comput. Methods Appl. Mech. Engrg., 48 (1985), pp. 313–327.

[10] P. L. Roe and D. Sidilkover, *Optimum positive linear schemes for advection in two and three dimensions*, SIAM J. Numer. Anal., 29 (1992), pp. 1542–1568.

[11] M. Rosenfeld and M. Israeli, *Numerical solution of incompressible flows by a marching multigrid nonlinear methods*, AIAA Journal, 25 (1987), pp. 641–647.

[12] D. Sidilkover, *Numerical solution to steady-state problems with discontinuities*, PhD thesis, The Weizmann institute of Science, Rehovot, Israel, 1989.

[13] D. Sidilkover and A. Brandt, *Multigrid solution to steady-state 2D conservation laws*, SIAM J. Numer. Anal., 30 (1993), pp. 249–274.

[14] I. Yavneh, *Multigrid Techniques for Incompressible Flows*, PhD thesis, Weizmann Institute of Science, Rehovot, Israel, 1991.

Level	Difference scheme			
	upwind	NC	ZC	TC
2	.517	.580	.570	.310
3	.232	.250	.252	$.910 \cdot 10^{-1}$
4	$.998 \cdot 10^{-1}$	.105	.106	$.233 \cdot 10^{-1}$
5	$.453 \cdot 10^{-1}$	$.465 \cdot 10^{-1}$	$.483 \cdot 10^{-1}$	$.583 \cdot 10^{-2}$

TABLE 5.2
L_1 error in u-velocity.